

Influence of two updated nuclear reaction rates on the evolution of low and intermediate mass stars

A. Weiss¹, A. Serenelli^{2,1}, A. Kitsikis¹, H. Schlattl¹, and J. Christensen-Dalsgaard³

¹ Max-Planck-Institut für Astrophysik, Karl-Schwarzschild-Str. 1, 85748 Garching, Federal Republic of Germany

² Institute for Advanced Study, Einstein Drive, Princeton, NJ 08540, USA

³ Institut for Fysik og Astronomi, Aarhus Universitet, Bygn. 520, Ny Munkegade, DK-8000 Aarhus C, Denmark

Abstract. Two key reactions of hydrostatic nuclear burning in stars have recently been revised by new experimental data – the $^{14}\text{N}(p, \gamma)^{15}\text{O}$ and 3α reaction rates. We investigate how much the new rates influence the evolution of low-mass, metal-poor and metal-free, stars and of an intermediate-mass star of solar-type composition. We concentrate on phases of helium ignition or thermally unstable helium burning. Our global result is that the new 3α rate has no significant influence on such stars, but that there is a noticeable, though small effect of the new $^{14}\text{N}(p, \gamma)^{15}\text{O}$ rate, in particular on the core helium flash and the blue loop during core helium burning in the intermediate-mass star.

Key words. Stars: interiors – Stars: evolution – Nuclear reactions

1. Introduction

The triple-alpha reaction is one of the key nuclear reactions for the synthesis of the elements in stars and is also the main energy source during helium burning. The reaction rate is dominated by resonances, the best known being the one at 7.65 MeV, theoretically predicted by Hoyle (1954), but there is considerable interest in determining all resonances with high precision. Recently, Fynbo et al. (2005) reported new measurements concerning resonances of ^{12}C with 3 α -particles obtained from ^{12}C -decay experiments. In particular, they found a dominant resonance at ≈ 11 MeV, while they did not confirm another at 9.1 MeV reported previously (Angulo et al. 1999). The new reaction rate (called the “ISOL” rate in the following) deviates from the one published by Angulo et al. (1999, NACRE): at temperatures between $2.5 \cdot 10^7$ and 10^8 K it is between 7 and 20% lower, but below $2.5 \cdot 10^7$ K up to 50% higher. The largest change occurs for $T > 3 \cdot 10^9$ K, where the new rate is increasingly lower by up to one order of magnitude (Fig. 1).

In the present paper we consider three cases of stellar evolution where a modified 3α rate might influence the models: the core helium flash in low-mass metal-poor stars, the core and shell helium burning in intermediate-mass stars of solar-like composition, and helium burning in metal-free low-mass stars. This mass range is interesting, because of the high temperature sensitivity during core and shell flashes, where instabilities amplify even small temperature variations.

Coincidentally, another key reaction has been re-determined recently by the LUNA collaboration, the $^{14}\text{N}(p, \gamma)^{15}\text{O}$ bottleneck reaction of the CNO-cycle (Formicola et al. 2004). The influence on globular cluster age determinations has already been discussed by Imbriani et al. (2004), and we will briefly comment on this. Our main interest, however, in this bottleneck reaction is again how stars of low and intermediate mass might be influenced in their evolution.

The outline of this paper is as follows: After describing briefly our stellar evolution code and the specific reaction rates for the 3α process and the ^{14}N reaction in Sect. 2, we present the results for the three stellar evolution cases described above in Sect. 3, followed by the conclusion in the final section.

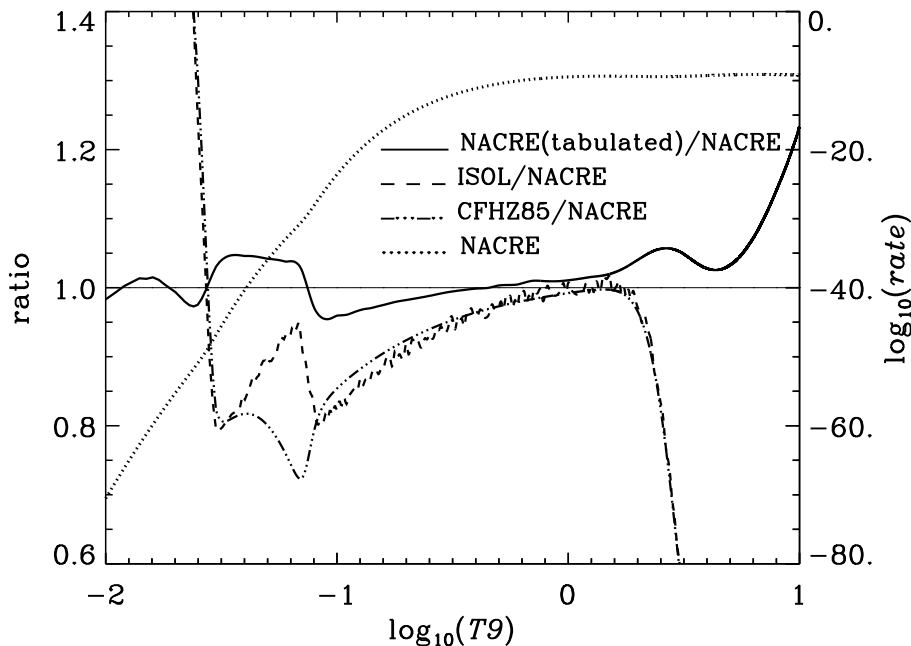


Fig. 1. 3α reaction rates relative to the NACRE analytic one (Angulo et al. 1999). Shown are the tabulated NACRE, CFHZ85 (Caughlan et al. 1985) and ISOL rates (Fynbo et al. 2005). The dotted line is the absolute value of the reference NACRE rate (scale on right axis).

2. Stellar evolution program

2.1. Basic properties

All calculations were done with the Garching stellar evolution code as described by Weiss & Schlattl (2000). The program was modified in only minor aspects since then. To summarize briefly the main physical ingredients, the code incorporates the OPAL equation of state (Rogers et al. 1996) and the OPAL opacity tables (Iglesias & Rogers 1996) supplemented by the molecular opacities of Alexander & Ferguson (1994). In the calculations presented here, the equation of state (EOS) of Irwin (see Cassisi et al. 2003) has been used, which is based on the OPAL EOS. Microscopic diffusion of all elements is implemented and has been included in the calculations of Sect. 3.2. Convection is treated according to standard mixing length theory with the Schwarzschild criterion for stability. Mass loss is included according to Reimers' formula (Reimers 1975), in the generalized form (Iben & Renzini 1983) containing a free scaling parameter η , which we will specify for each case.

Nuclear burning is taken into account by a network which treats hydrogen and helium burning separately, unless both protons and α -particles are present and temperatures are high enough for helium processing. In such cases (see Sect. 3.2) the whole network and any mixing process are treated simultaneously. For details on this see Schlattl et al. (2001).

2.2. $^{14}\text{N}(p, \gamma)^{15}\text{O}$ and 3α rate

The standard implementation of the first rate¹ is according to the recommendation in Adelberger et al. (1998, Table VI; hereafter referred to as Adel98), with the astrophysical $S(0)$ -factor being 3.5 keV b. NACRE (Angulo et al. 1999) gives $S(0) = 3.2 \pm 0.8$ keV b. The new LUNA value (Formicola et al. 2004) is 1.7 ± 0.1 (stat) ± 0.2 (sys) keV b; $S'(0)$ and $S''(0)$ have been left unchanged at the Adelberger values and the new rate therefore differs from the old one by a constant factor. This is in agreement with the procedure of Imbriani et al. (2004).

The standard implementation of the 3α rate in our program is the analytic form of Caughlan et al. (1985, CFHZ85). Since Fynbo et al. (2005) used the analytic fit to the NACRE rate for reference, we implemented the same rate for the comparisons. The new ISOL rate was available to us in tabulated form (Chr. Diget, private communication). Fig. 1 shows all 3α rates compared with the NACRE analytic rate. Note that in the temperature range of interest to us the new rate lies within the uncertainty of the NACRE rate (Angulo et al. 1999) and that the analytic fit of the NACRE rate deviates from the tabulated values by up to 5%. The ISOL rate agrees quite well with that of Caughlan et al. (1985) over an extended range below temperatures of several billion degree. The critical temperature above which helium burning is taken into account was set to $5 \cdot 10^7$ K; using still lower values has no influence on the models.

3. Sample calculations

3.1. Core helium flash in a Pop. II star

In this section we present the results of our sample calculations and compare them with reference calculations that use the NACRE and Adel98 rates for the 3α and $^{14}\text{N}(p, \gamma)^{15}\text{O}$ reaction rates, respectively. We begin with the onset of helium burning in stars of low mass and degenerate helium cores, the so-called core helium flash. We performed calculations for two masses, $0.8 M_{\odot}$ and $1.0 M_{\odot}$, and three metallicities, $Z = 0.001, 0.0001, 0.00001$ and initial helium content $Y = 0.25$. No mass loss was assumed. The calculations were started from the zero-age main sequence (ZAMS) and followed through the flash until the star settles on the horizontal branch (HB) and then up to the early AGB.

Updating the 3α rate, the changes are very small but as would be expected from a slightly lower rate. The tip of the RGB is almost unchanged, the luminosity being 2% higher for the new rate. The core mass increases very little, between 0.002 and $0.003 M_{\odot}$ depending on mass and metallicity. The age of the models also increases by a mere 0.2 Myr at most. We show the resulting tracks in the Hertzsprung-Russell Diagram (HRD) in Fig. 2 for the lowest metallicity and mass, and list a few quantities in Table 1. Note that even the secondary flashes during the settling to the HB are almost indistinguishable. The agreement between the two cases is as close for all other cases.

We then varied the $^{14}\text{N}(p, \gamma)^{15}\text{O}$ rate ($3\alpha = \text{NACRE}$). The effect turned out to be much larger, and can be seen in Fig. 2 (lower panel). We notice differences already around the turn-off, and in particular during

¹ The term "rate" is to be understood as $N_A^{(n-1)} \langle \sigma v \rangle$, that is as the Maxwellian-averaged reaction rate (see Angulo et al. 1999) in units of $\text{cm}^3 \text{mol}^{-1} \text{s}^{-1}$ for n reaction partners.

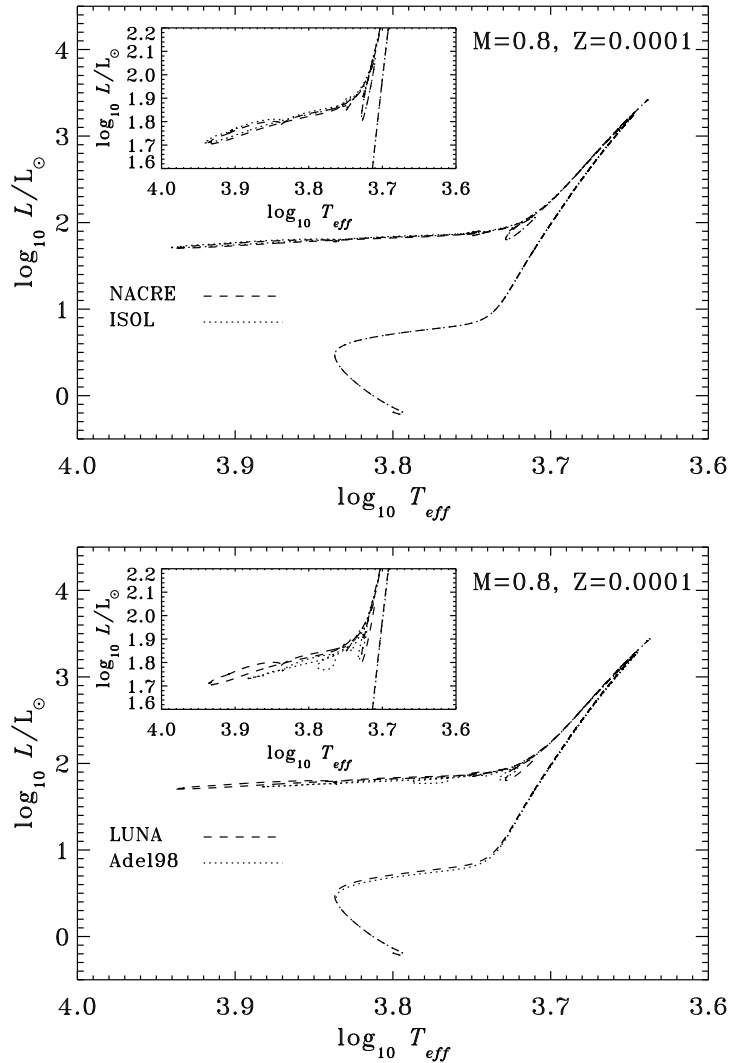


Fig. 2. Evolution of a stellar model of $0.8 M_{\odot}$ and $Z = 10^{-4}$ from ZAMS to HB. In the upper panel we varied the 3α - and in the lower one the $^{14}\text{N}(p, \gamma)^{15}\text{O}$ -rate. The insets show the approach to the HB in greater detail.

the approach to the HB; the effective temperature of the zero-age HB model increases by up to 20% for the LUNA rate.

At this point it is worthwhile to clarify the result found by Imbriani et al. (2004). They showed that due to the improved $^{14}\text{N}(p, \gamma)^{15}\text{O}$ rate the ages of globular clusters increase by up to 1 Gyr. This is not simply due to the slower bottleneck reaction leading to longer timescale for hydrogen fusion. In Fig. 3 we display for one example ($1 M_{\odot}$, $Z = 0.001$) the evolution of luminosity and effective temperature during main-sequence and red-giant-branch evolution. Evidently, the luminosity evolution on the main sequence is hardly affected by the nuclear rate. Energy generation takes place within a core that has a temperature only marginally higher but is more extended as the result of a shallower temperature profile. So, while at the center hydrogen is burning at a slower pace (same T , lower reaction rate), more mass is involved in the nuclear fusion. The time it takes to deplete hydrogen in the core is therefore somewhat higher (in our case +190 Myr), but the exhausted core is larger (+0.013 M_{\odot}). Due to that larger core mass, towards the end of the main sequence the central temperature is higher by approximately 5% for the LUNA rate. Another consequence of the different core evolution is a modified temperature gradient, and thus T_{eff} at the end of the main sequence evolves differently (Fig. 3), influencing the turn-off luminosity which is defined as the value of L at the bluest point along the MS track. To be more quantitative, the turn-off in the case of the Adelberger rate is at $t = 4.38$ Gyr, $\log T_{\text{eff}} = 3.852$, and $\log L/L_{\odot} = 0.554$. For the revised LUNA rate the hottest point is reached later, at $\log T_{\text{eff}} = 3.854$, when $\log L/L_{\odot} = 0.593$ and $t = 4.62$ Gyr, an increase of 240 Myr. Note, however, that at the turn-off age of the Adelberger case, $T_{\text{eff}} = 3.854$ and $\log L/L_{\odot} = 0.558$ for LUNA, i.e., almost identical. Thus, the change in

Table 1. Selected properties of one of our Pop. II models ($M = 0.8 M_{\odot}$; $Z = 10^{-4}$) at critical stages of its evolution from ZAMS to ZAHB evolved with various combinations of reaction rates as shown in Fig. 2. M_{He} is the helium core mass in solar unit at the helium flash.

$^{14}\text{N}+\text{p}$:		Adel98	LUNA	
3α :		NACRE	NACRE	ISOL
Turn off	$\log L/L_{\odot}$	0.437	0.467	0.467
	$\log T_{\text{eff}}$	3.8360	3.8368	3.8368
	Age[Myr]	11130	11273	11273
RGB-tip	$\log L/L_{\odot}$	3.285	3.237	3.246
	$\log T_{\text{eff}}$	3.6449	3.6479	3.6474
	M_{He}	0.4990	0.5052	0.5074
	Age[Myr]	12638	12699	12699
ZAHB	$\log L/L_{\odot}$	1.744	1.715	1.722
	$\log T_{\text{eff}}$	3.8614	3.9324	3.9344

the turn-off is due to the modified interior structure, which influences the morphology of the evolutionary track. We have also investigated a few other cases and find that at even lower metallicity ($Z = 0.0001$) the age differences decrease to 1-2%.

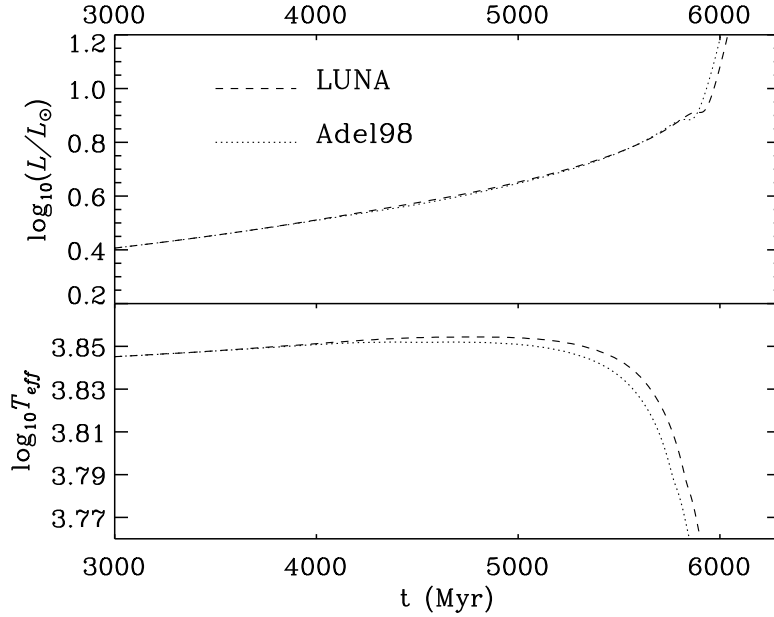


Fig. 3. Comparison of luminosity and effective temperature as functions of time (in Myr) for a star with $1 M_{\odot}$ and $Z = 0.001$, calculated with both the Adelberger (dotted line) and LUNA (dashed line) $^{14}\text{N}(p, \gamma)^{15}\text{O}$ rate.

3.2. Core helium flash in a Pop. III star

A particularly interesting variant of the core helium flash is that found in metal-free (Pop. III) stars. Details on this subject were provided by Weiss et al. (2000) and Schlattl et al. (2001). We have calculated the evolution of a star of $M = 1 M_{\odot}$, $Y_i = 0.23$ ($Z = 0$). We varied both rates as before, the reference case using the Adelberger et al. (1998) $^{14}\text{N}(p, \gamma)^{15}\text{O}$ and NACRE 3α rates. Some properties of the models are listed in Table 2. We also investigated the case “LUNA + CFHZ85”, but do not discuss it further, because it is indistinguishable from the “LUNA + ISOL” case.

The first particularity of Pop. III evolution is a loop in the HRD after the main sequence, which is due to spurious carbon production in the hot core and the ignition of the CNO-cycle (for details see Weiss et al. 2000). The presence of this loop depends on the stellar mass; it is present in our reference case, but vanishes in all cases with the new (lower) LUNA rate for $^{14}\text{N}(p, \gamma)^{15}\text{O}$. As the reason for the disappearance of the loop we identify the fact that the lower CNO-luminosity prevents the creation of a convective core, which otherwise leads to an increase of the hydrogen abundance in the core and thus to a luminosity enhancement. We note that the creation of the first in-situ carbon nuclei is not influenced by the choice of the 3α rate.

Table 2. Selected properties of Pop. III models evolved with various combinations of reaction rates. We list luminosity and helium core mass at the onset of the first and second core helium flash, as well as the maximum helium luminosity ($\log L_{\text{He}}^{\text{max}}/L_{\odot}$) and the mass at which the maximum temperature is reached ($M_{\text{Tmax}}/M_{\odot}$) at the time of $\log L_{\text{He}}^{\text{max}}/L_{\odot}$. In addition, the surface abundances (mass fractions) after the flash-induced mixing event is given for key elements.

$^{14}\text{N}+p$		Adel98	LUNA	
3α		NACRE	NACRE	ISOL
MS	CN-loop	yes	no	no
	$\log(L/L_{\odot})$	2.324	2.302	2.311
1 st flash	$\log(L_{\text{He}}^{\text{max}}/L_{\odot})$	10.08	10.01	10.03
	M_{He}/M_{\odot}	0.4784	0.4755	0.4780
	$M_{\text{Tmax}}/M_{\odot}$	0.1849	0.1818	0.1863
	H	0.5288	0.5369	0.5366
	He	0.4582	0.4510	0.4510
dredge up	^{12}C	0.00417	0.00292	0.00302
	surface	^{13}C	0.00111	0.00080
abdc.	^{14}N	0.00772	0.00837	0.00861
	^{15}N	$2.6 \cdot 10^{-7}$	$1.1 \cdot 10^{-7}$	$1.1 \cdot 10^{-7}$
	^{16}O	$3.9 \cdot 10^{-6}$	$3.4 \cdot 10^{-6}$	$4.0 \cdot 10^{-6}$
		$\log(L/L_{\odot})$	3.532	3.487
2 nd flash	$\log(L_{\text{He}}^{\text{max}}/L_{\odot})$	9.592	9.764	9.770
	M_{He}/M_{\odot}	0.4585	0.4615	0.4638
	$M_{\text{Tmax}}/M_{\odot}$	0.0789	0.0665	0.0729

The second particular event is the (first) core helium flash that happens at a much lower luminosity in Pop. III stars than in those with $Z \gtrsim 10^{-6}$, due to the higher core temperature. As the H-shell temperatures are higher as well, the so-called entropy barrier is lower and a mixing event between the hydrogen-rich envelope and the hot carbon-enriched helium layers is possible (see also Fujimoto et al. 2000). As a consequence, the envelope will be enriched drastically in CNO-products and helium (see Table 2). As in the case of ordinary Pop. II stars, the new 3α rate has only a very moderate influence on the flash: it starts at slightly higher luminosity and core mass, but the increase is not significant. The peak helium luminosity $L_{\text{He}}^{\text{max}}$ is unchanged, within the computational uncertainties.

In contrast, the new $^{14}\text{N}(p, \gamma)^{15}\text{O}$ rate has a much stronger influence. The flash luminosity is lower due to the higher shell temperatures and the core mass is higher. This is probably a consequence of the fact that the core mass-luminosity relation depends on the temperature exponent of the shell hydrogen burning. For CNO-burning, it is $L \propto M_c^7$, and for pp -burning $\propto M_c^3$. Very metal-poor stars have a very small contribution from the CNO-cycle only and therefore follow closely the latter relation. A lower $^{14}\text{N}(p, \gamma)^{15}\text{O}$ rate leads to a smaller temperature exponent, and thus the core mass is slightly higher at given luminosity.

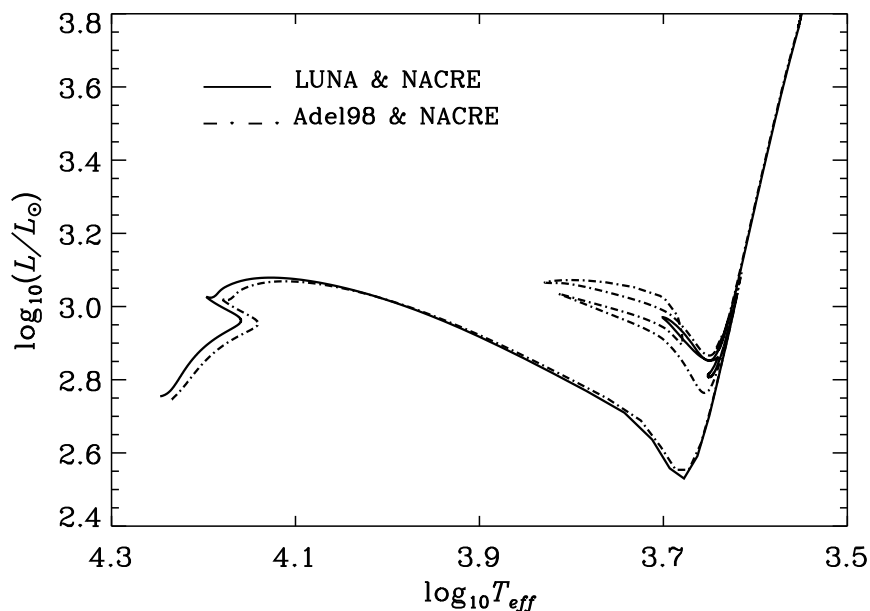


Fig. 4. Evolution in the HRD for the Pop. I model with $M = 5 M_{\odot}$, showing the influence of changing the $^{14}\text{N}(p, \gamma)^{15}\text{O}$ reaction rate. The two cases are indicated in the figure.

The result of the flash-induced dredge-up shows larger (relative) variations (Table 2), but with no apparent systematics, except that in the table the dredge-up appears generally to be stronger for the older rates, while for the latest rate more CN-burning could take place.

After the star has settled again on the giant branch, it resumes its evolution since core helium burning has been extinguished as a result of the first flash and mixing. A second, more moderate flash appears at a standard RGB tip luminosity ($\log L/L_{\odot} \approx 3.5$). Table 2 demonstrates again that the largest changes are due to the new LUNA $^{14}\text{N}(p, \gamma)^{15}\text{O}$ rate, leading to lower ignition luminosity but higher helium core mass. The largest variation found in Table 2 is therefore between the reference case (col. 3) and that updating the $^{14}\text{N}(p, \gamma)^{15}\text{O}$ rate only (col. 4).

3.3. Helium burning and thermal pulses in a Pop. I star

As a third case we have investigated that of a typical solar-metallicity intermediate-mass star evolving into and through the Asymptotic Giant Branch (AGB) phase. The composition of our model was $X = 0.695$, $Y = 0.285$ and $Z = 0.02$. Mass loss according to Reimers was taken into account with the scaling parameter η being 0.4 on the RGB and 0.5 on the AGB.

In Fig. 4 we show the evolution of this model in the HRD for the two $^{14}\text{N}(p, \gamma)^{15}\text{O}$ reaction rates. Using the updated LUNA rate the main-sequence evolution takes place at higher temperatures, implying a more compact structure of the model. This is similar to the Pop. II model (Sect. 3.1) but more pronounced. As the evolution of intermediate mass stars is very sensitive to the internal composition profile, the consequences for the core helium burning phase are quite large: the blue loop gets significantly shorter.

The luminosity variations during the thermal pulses (TP) along the AGB are shown in Fig. 5. The TPs start earlier by about 1 million years for the LUNA rate, which is due to a shorter main-sequence lifetime. We have therefore shifted the time axis for the Adel98 case to coincide at the pre-flash luminosity maximum. The pulse behaviour is similar, although the peak luminosity and peak helium luminosity (not shown) are higher, and the interpulse duration longer for the new LUNA rate. This is consistent with earlier findings concerning the influence of H-burning rates on pulse behaviour (Despain & Scalo 1976), and in particular with the recent investigation by Herwig & Austin (2004), who found stronger flashes for lower $^{14}\text{N}(p, \gamma)^{15}\text{O}$ rates in a $2 M_{\odot}$ model. These differences become smaller with increasing pulse number. We followed 15 (LUNA) respectively 8 (Adel98) pulses and then stopped the calculations.

Using the new LUNA $^{14}\text{N}(p, \gamma)^{15}\text{O}$ reaction rate, we then compared models calculated with the three variants of the 3α rate. Again, the blue loops, being most sensitive to structure variations, show the clearest

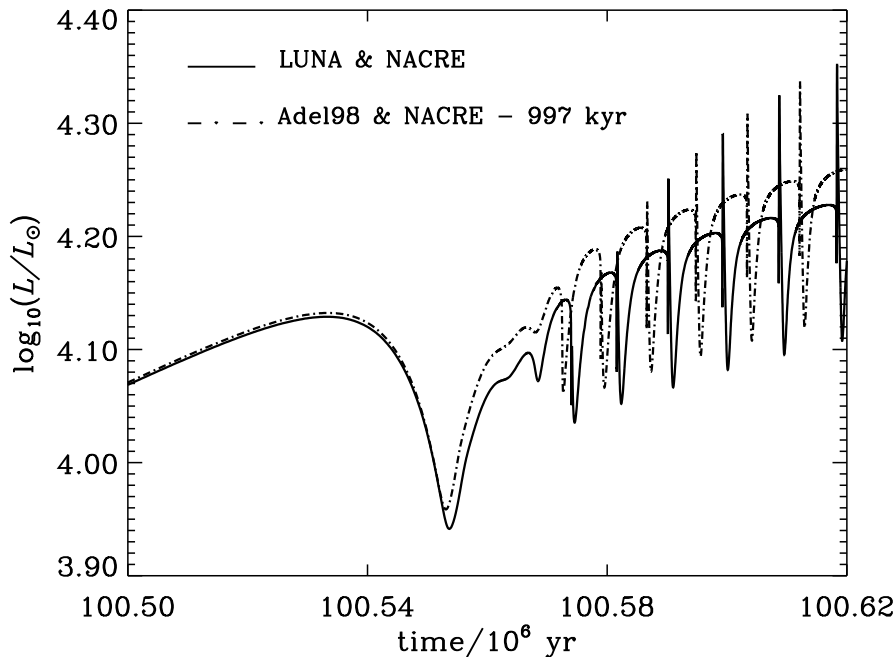


Fig. 5. Thermal pulses on the AGB for two different $^{14}\text{N}(p, \gamma)^{15}\text{O}$ reaction rates. Shown is the total luminosity as function of time (in million years). To display better the differences the time axis for the Adel98 $^{14}\text{N}(p, \gamma)^{15}\text{O}$ case has been shifted by -997 kyr.

reaction, and get even shorter for the new ISOL rate. Concerning the thermal pulses, they are extremely similar to each other, and if shifted by -80 kyr for the CFHZ85 and -67 kyr for the new ISOL 3α rate relative to the NACRE case they completely agree.

Finally, we mention the chemical composition of all cases investigated in terms of central carbon and oxygen abundance after core helium burning. The carbon abundance ranges from 0.200 to 0.223 with the highest value reached for the older reaction rates. Consequently the core most rich in oxygen is obtained for the LUNA $^{14}\text{N}(p, \gamma)^{15}\text{O}$ and new 3α rates combined. However, in spite of noticeable variations, they are minor compared with the uncertainties still present due to the $^{12}\text{C}(\alpha, \gamma)^{16}\text{O}$ rate. As an example, we quote here the result of Bono et al. (2000, their Tab. 6) that the time spent in the blue loop by a $5 M_{\odot}$ star changes by up to 2.12 Myr (33%), the mass of the CO-core by $0.26 M_{\odot}$ (5%), and the C/O ratio by a factor of 3 when varying the rate within a factor of 2.3, which is comparable to the rate uncertainty (Kunz et al. 2002).

4. Conclusions

We have investigated the influence of new rates for the $^{14}\text{N}(p, \gamma)^{15}\text{O}$ and 3α reactions on the evolution of low- and intermediate-mass stars, considering cases in which helium burning proceeds under thermally unstable conditions. In all cases we find negligible changes in the evolution and also in the interior evolution due to the new 3α rate. The RGB tip brightness is slightly increased due to the lower rate at very low temperatures corresponding to the earliest phases of helium ignition. The largest effect shows up in the blue loops during core helium burning of the $5 M_{\odot}$ star, emphasizing the sensitivity of these loops to details of the interior structure.

The $^{14}\text{N}(p, \gamma)^{15}\text{O}$ rate has a definitely stronger influence. It prolongs the duration of central hydrogen burning, increases the turn-off temperature and thus indirectly the turn-off location, it leads to a disappearance of the CN flash in the Pop. III post-main-sequence star, strongly reduces the blue loop during core helium burning of a $5 M_{\odot}$ star, and also influences the thermal pulses. Interestingly, these are, apart from a very minor shift in time, almost identical in the case of varying the 3α rate.

We conclude that the new 3α rate has no influence on the evolution of low and intermediate-mass stars, and that the effect of the LUNA $^{14}\text{N}(p, \gamma)^{15}\text{O}$ is tiny, but noticeable. Further investigations into its effect on more massive stars as well as of the effect of the 3α rate on massive stars are indicated. If the differences in the various rate determinations we have used are representative of the experimental errors, then both rates are no longer a source of uncertainty for stellar modeling.

Acknowledgements. We thank Chr. Diget for making available the rate table. F. Meissner kindly provided data for the turn-off values of metal-poor stars, and F. Herwig information about his AGB-models with the new rates. A.W. is grateful to L. Girardi for explanations concerning the core mass-luminosity relation. A.M.S is supported in part by NSF grant PHY-0070928.

References

- Adelberger, E., Austin, S., Bahcall, J., et al. 1998, *Rev. Mod. Phys.*, 70, 1265
Alexander, D. R. & Ferguson, J. W. 1994, *ApJ*, 437, 879
Angulo, C., Arnould, M., Rayet, M., et al. 1999, *Nucl.Phys. A*, 656, 3
Bono, G., Caputo, F., Cassisi, S., et al. 2000, *ApJ*, 543, 955
Cassisi, S., Salaris, M., & Irwin, A. 2003, *ApJ*, 588, 862
Caughlan, G., Fowler, W., Harris, H., & Zimmerman, B. 1985, *Atomic Data and Nuclear Data Tables*, 32, 197
Despain, K. & Scalo, J. 1976, *ApJ*, 208, 789
Formicola, A., Imbriani, G., Costantini, H., et al. 2004, *Phys. Lett. B*, 591, 61
Fujimoto, M. Y., Ikeda, Y., & Iben, I. 2000, *ApJL*, 529, L25
Fynbo, H., Diget, C., Bergemann, U., et al. 2005, *Nature*, 433, 136
Herwig, F. & Austin, S. 2004, *ApJL*, 613, L73
Hoyle, F. 1954, *ApJS*, 1, 121
Iben, I. & Renzini, A. 1983, *ARA&A*, 21, 271
Iglesias, C. A. & Rogers, F. J. 1996, *ApJ*, 464, 943
Imbriani, G., Costantini, H., Formicola, A., et al. 2004, *A&A*, 420, 625
Kunz, R., Fey, M., Jaeger, M., et al. 2002, *ApJ*, 567, 643
Reimers, D. 1975, *Mem. Soc. Roy. Sci. Liège*, 8, 369
Rogers, F. J., Swenson, F. J., & Iglesias, C. A. 1996, *ApJ*, 456, 902
Schlattl, H., Cassisi, S., Salaris, M., & Weiss, A. 2001, *ApJ*, 559, 1082
Weiss, A., Cassisi, S., Schlattl, H., & Salaris, M. 2000, *ApJ*, 533, 413
Weiss, A. & Schlattl, H. 2000, *A&A Supplement*, 144, 487